JOC The Journal of Organic Chemistry

Article

pubs.acs.org/joc

8-Amino-BODIPYs: Structural Variation, Solvent-Dependent Emission, and VT NMR Spectroscopic Properties of 8-R_2N-BODIPY

Robinson I. Roacho,[†] Alejandro Metta-Magaña,[†] Michelle M. Portillo,[†] Eduardo Peña-Cabrera,[‡] and Keith H. Pannell*,[†]

[†]Department of Chemistry, The University of Texas at El Paso, El Paso, Texas 79968-0513, United States

[‡]Universidad de Guanajuato, Noria Alta S/N, Guanajuato, GTO, 36050, Mexico

Supporting Information

ABSTRACT: New 8-NR_2-BODIPYs, R_2 = H^{i}Pr (**3a**), H^{i}Bu (**3b**), and Et_2 (**4**), are reported. Restricted rotation about the C8−N bond in such molecules has been observed for the first time (**3a** and **3b**) and evaluated using VT NMR. The fluorophores **3a** and **3b** are blue emitters, and the efficiency of the emission is closely related to the polarity of the solvent, e.g., hexane > toluene > DCM > THF > MeOH > H_2O, an effect also noted by emission variation in alcohol solvents $H(CH_2)_nOH$, n = 1−6. In mixed-solvent systems, addition of 10−15% of the more polar solvent results in transformation of the emission properties to those of the bulk polar solvent. Compound **4** has zero emission in all solvents. The crystal structures of **3a**, **3b**, and **4** are reported, along with that of the parent 8-NH_2-BODIPY (**2**). Compounds **2**, **3a**, and **3b** exhibit trigonal planar N atoms which are coplanar with the BODIPY core; **4** exhibits a very significant distortion that breaks the planarity of the extended BODIPY π system due to the steric impact of the two ethyl groups, an observation that explains the lack of emission for **4**.

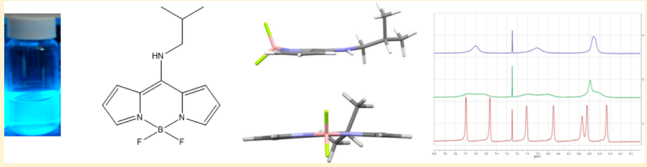

INTRODUCTION

BODIPY dyes have been extensively studied since such molecules possess applications in the areas of protein taggers,[1] laser dyes,[2] metal sensors,[3,4] and probes for anions.[5] This range of utility is due to the capacity to substitute the many positions of the core structure, Figure 1, thereby tweaking both its optical and binding characteristics.

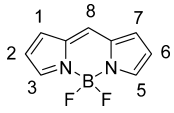

Figure 1. BODIPY core.

BODIPY compounds generally exhibit a high fluorescence intensity in the 500 nm range (green), but judicious choice of electronic substituents can result in yellow, red, and near-IR fluorescence emission.[6] In general, a bathochromic shift is observed in both excitation and emission wavelengths (with respect to the parent BODIPY) when the π-system conjugation is further expanded, for example, by allyl and aryl groups.[6] One of us has recently described a series of 8-amino BODIPYs which exhibit a hypsochromic shift that results in a blue emission and a high laser efficiency.[7−9] An interesting feature of these new amino materials is that their properties seem to depend upon both the size and electronic character of the substituents on the N atom. A hemicyanine, **B** in Figure 2, resonance contribution to the overall structure results in significant delocalization of the N lone pair to the BODPY core,

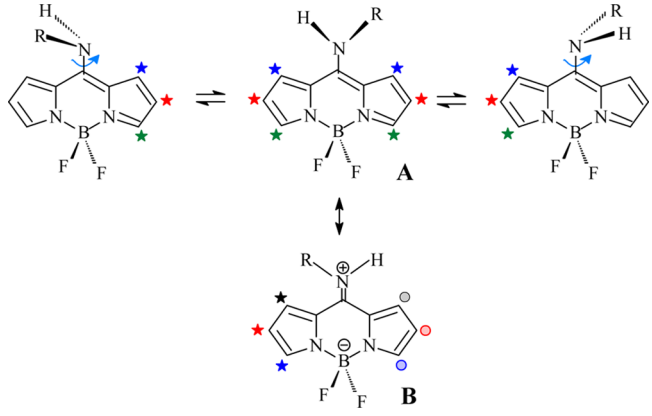

Figure 2. Rotation on C−N bond inducing asymmetry in the molecule illustrating the equivalence or nonequivalence of the positions via color.

especially in the excited state.[8] This feature was held responsible for the observed blue shifts. Additionally, introduction of electron-releasing alkyl groups on the N atom further enhances blue emission by destabilizing the LUMO of the dyes. On the other hand, the bulk of such alkyl substituents will retard the stability of the hemicyanine since a planar R_2N required for the lone pair delocalization is not possible for larger groups.

Received: January 8, 2013
Published: April 1, 2013

   dx.doi.org/10.1021/jo302758a | J. Org. Chem. 2013, 78, 4245−4250

In an extension of this chemistry, we now report the synthesis of new 8-R_2N-BODIPYs, R_2 = H^{i}Pr, H^{i}Bu, and Et_2, spectroscopic characterization including VT NMR illustrating such restricted rotation about the C8−N bond for the first time, their solvent dependent emission properties, and single crystal structures which provide significant insight into their varying emission efficiency resulting from rupture of the delocalized π system.

RESULTS AND DISCUSSION

Synthesis of 8-Amino-BODIPYS. The reaction between 8-methylthio-BODIPY (**1**) and the three amines reported herein, ^{i}PrNH$_2$, ^{i}BuNH$_2$, and Et_2NH, was extremely facile and produced the new 8-amino-BODIPYs in very high yield, eq 1.[8,10]

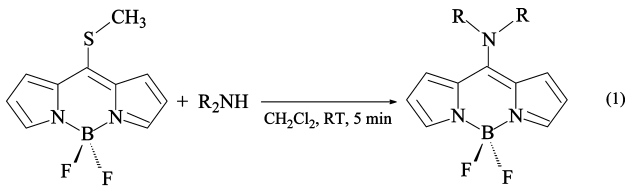

R_2 = H_2 (**2**); (^{i}Pr)H (**3a**); (^{i}Bu)H (**3b**); Et_2 (**4**)

Simple mixing of **1** and 20% excess of the amine in dichloromethane and stirring for 5 min resulted in complete reaction such that removal of the solvent and excess amine followed by recrystallization of the products from a (4:1) hexane/methylene chloride solvent mixture resulted in a high yield (∼90%) of the product.

NMR Characterization of 8-Amino-BODIPYS. Previously reported secondary amino BODIPYs, (methylamino- (MeNH-) and propargylamino- ($HCCCH_2NH$)-BODIPY compounds exhibited the nonequivalence of the six pyrrole hydrogen atoms by ^{1}H NMR in polar solvents but equivalent protons in $CDCl_3$.[7−9] This was explained by suggesting a rotation about the C8−N bond such that an orientation of the N-substituents in parallel to the plane of the BODIPY core could be formed, species **A** in Figure 2; however, no experimental proof for such a restricted rotation was reported. This rotamer **A** could permit the N-lone pair to be delocalized into the π-system of the BODIPY core with the resultant hemicyanine tautomer **B** being the important contribution to the structure which could be stabilized in polar solvents.

Unlike the previous 8-*sec*-amino-BODIPYs the ^{1}H NMR spectra for compounds **3a** and **3b** exhibits six resonances in the aromatic region in $CDCl_3$ as well as in polar solvents, corresponding to a non-symmetric molecule, Figure 3. However, in $CDCl_3$ these resonances are broad whereas in MeOD they are sharp, as expected for the stabilization of the highly polar hemicyanine structure. This observation suggests that in the relatively nonpolar $CDCl_3$ solvent the isopropyl and isobutyl groups induce enough steric hindrance to result in a restricted rotation about the C8−N bond thus reflecting an equilibrium between rotamers. Indeed, variable-temperature ^{1}H NMR studies on **3a** and **3b** in $CDCl_3$ confirmed this suggestion since at 5 °C the spectra illustrated six sharp peaks, Figure 4. Progressively raising the temperature results in a broadening and final coalescing of the six resonances into three singlets as expected for a now rapid rotation about the C8−N bond. This classic behavior confirms the concept of rotation about the C8−N bond, and we obtain activation energies of 59.2 and 62.9 kJ/mol for the isopropyl- and isobutylamino-BODIPYs, respectively.

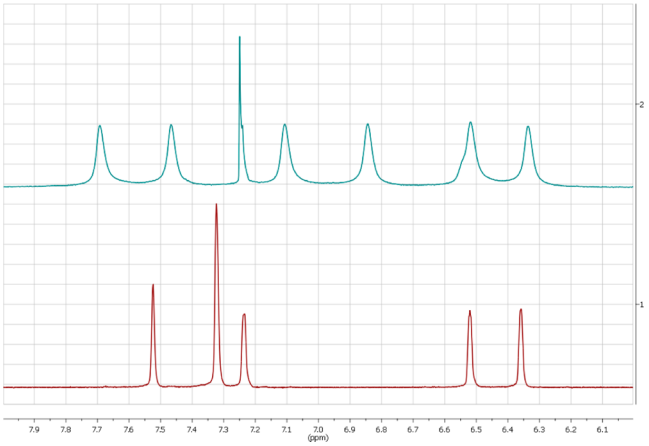

Figure 3. Aromatic region of ^{1}H NMR spectrum of **3b** in $CDCl_3$ (top) and CD_3OD (bottom) at ∼25 °C. Note: in the $CDCl_3$ spectrum, the NH has been exchanged with ND via treatment with CD_3OD and is not present as it is in Figure 4. In the CD_3OD spectrum there is an overlap of two resonances at 7.3 ppm .

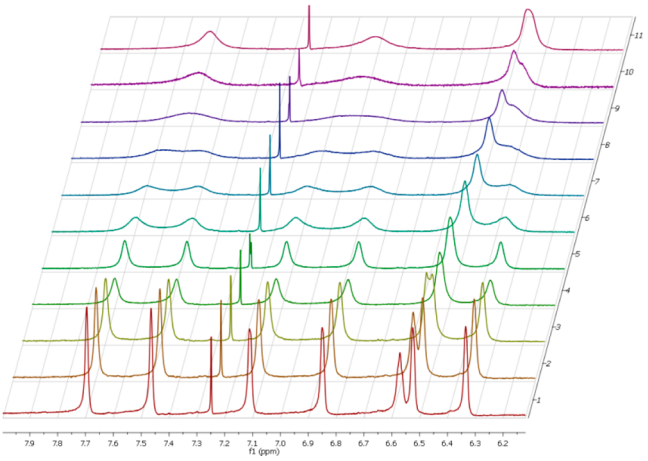

Figure 4. Aromatic region ^{1}H NMR spectra of **3b** in $CDCl_3$ from 55 °C (top) to 5 °C (bottom). The extra resonance at ∼6.6 ppm is due to the NH.

In the case of **4**, where there is no asymmetry associated with a disubstituted amine, only three resonances are expected in the ^{1}H NMR spectrum regardless of solvent, and this is in accord with the spectra obtained over the same range of temperature used for the analysis of **3**. As expected a similar NMR pattern with three resonances was noted for the 8-H_2N-BODIPY, **2**. The ^{19}F NMR spectra of **3a**, **3b**, and **4** exhibit the typical quartet signal noted for other reported BODIPYs, close to the typical chemical shift of −146 ppm.[11,12]

Optical Properties of 8-Amino-BODIPYS. Each of the new amino-BODIPYs exhibits a yellow color in solution and the solid state, in contrast to the red color of the starting material **1**.[10] The UV/vis spectral properties of the new compounds **3a** and **3b** are recorded in Table 1. Each exhibits an absorbance in the range 400−430 nm, with molar extinction coefficients ∼120000. For both compounds, this absorbance exhibits a small progressive hypsochromic shift as the solvent polarity is increased as noted before.[8]

dx.doi.org/10.1021/jo302758a | J. Org. Chem. 2013, 78, 4245−4250

Table 1. Summary of Optical Features of 3a and 3b[a]

	3a			3b			2			4
solvent	absorbance λ_{max}, nm (ε, M^{-1} cm^{-1})	emission λ_{max}, nm	φ	absorbance λ_{max}, nm (ε, M^{-1} cm^{-1})	emission (λ_{max}, nm)	φ	absorbance λ_{max}, nm (ε, M^{-1} cm^{-1})	wmission λ_{max}, nm	φ	absorbance λ_{max}, nm (ε, M^{-1} cm^{-1})
hexane	412 (1.09)	472	0.98	413 (1.21)	462	1.00	428 (0.98)	456	0.96	427 (0.97)
toluene	412 (1.29)	474	0.93	413 (1.34)	460	0.92	426 (1.01)	450	0.98	424 (1.02)
DCM	408 (1.23)	468	0.80	411 (1.44)	456	0.86	406 (1.02)	440	0.97	416 (0.99)
THF	406 (1.13)	462	0.16	406 (1.21)	450	0.26	404 (1.01)	436	0.95	414 (1.05)
Acetone	401 (1.13)	460	0.04	402(1.25)	449	0.06	399 (1.15)	435	0.97	400 (1.03)
MeOH	401 (1.08)	464	0.02	397 (1.22)	446	0.04	395 (1.12)	435	0.92	398 (0.98)

[a] ε is given as log 10^5.

The emission spectra of **3a** and **3b** exhibit a band between 446 and 472 cm^{-1}, which also exhibit a small hypsochromic shift with increasing solvent polarity similar to the absorbance spectra. The resulting Stokes shifts are thus equivalent in all solvents, ~60 cm^{-1}. More dramatic than these small shifts are large changes in emission efficiency, especially for **3a** and **3b,** as a function of solvent, illustrated in Figure 5, which presents a range of normalized emission intensities ranging from 1.0 in hexane to 0.06 in MeOH.

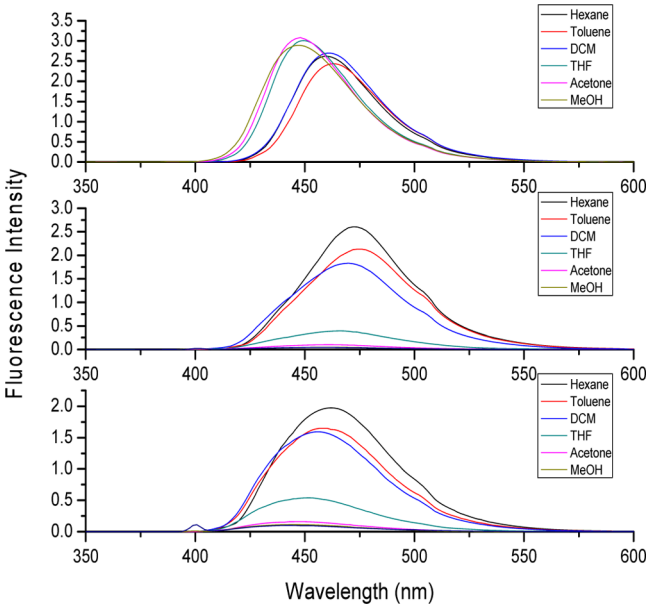

Figure 5. Emission spectrum of **2** (top), **3a** (middle), and **3b** in different solvents at 1 μM solutions.

This significant solvent dependency can be further illustrated by progressive alteration of solvent compositions. Thus, systematic change from a DCM/MeOH solvent composition of 100% DCM to 100% MeOH results in the normalized emission variations noted in Figure 6 for both **3a** and **3b**. Dramatically the emission for **3a** and **3b** in a solvent mixture of DCM/MeOH with a mole fraction of DCM of 0.85 results in an emission intensity equivalent to that observed in pure MeOH.

We performed the same set of experiments using $CHCl_3$/THF and $CHCl_3$/acetonitrile and THF/water mixtures and observed similar emission changes, illustrating the generality of the process, Figure S13 (Supporting Information). The results using the latter solvent system provided no evidence for an enhanced emission at high mole fractions of H_2O which in other studies have been taken as indicators of aggregation-induced emission.[13]

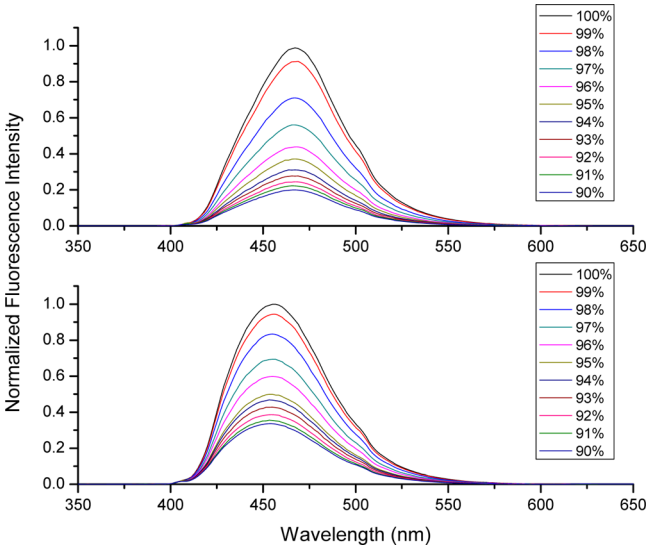

Figure 6. Emission of 1 μM solutions of **3a** (top) and **3b** (bottom) DCM/MeOH solvent gradient system.

A further demonstration of the sensitivity of **3a** and **3b** is presented in Figure 7, where the emission is noted as a response to varying the polarity of the alcohol used as solvent, $H(CH_2)_nOH$ (n = 1–6). The increasing hydrophobicity of the

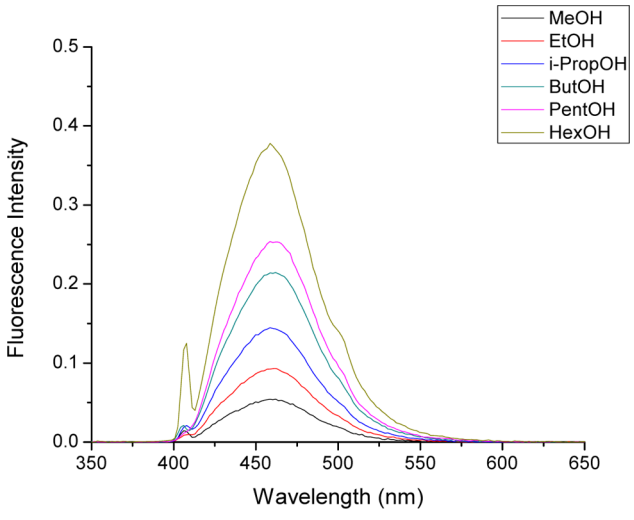

Figure 7. Solutions of **3a** (1 μM) in different alcohols.

dx.doi.org/10.1021/jo302758a | J. Org. Chem. 2013, 78, 4245–4250

Table 2. Selected Bond Distances for the BODIPY Core in 2−4

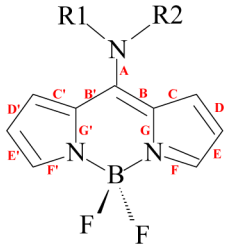

1 R1 = R2 = H
2 R1 = H; R2 = ^{i}Pr
3 R1 = H; R2 = ^{i}Bu
4 R1 = R2 = Et

bond	2	3a1	3a2	3b1	3b2	4
A	1.332(4)	1.315(7)	1.314(6)	1.324(8)	1.347(8)	1.338(4)
B	1.419(5)	1.427(8)	1.409(7)	1.420(8)	1.415(7)	1.456(5)
B′	1.424(5)	1.416(8)	1.430(7)	1.441(8)	1.452(8)	1.445(5)
C	1.391(5)	1.427(8)	1.384(7)	1.396(8)	1.393(8)	1.404(5)
C′	1.395(5)	1.358(7)	1.36(7)	1.441(8)	1.372(8)	1.416(5)
D	1.394(6)	1.366(7)	1.364(8)	1.390(9)	1.370(7)	1.388(5)
D′	1.384(6)	1.366(8)	1.369(7)	1.359(8)	1.375(8)	1.390(5)
E	1.377(6)	1.359(8)	1.363(8)	1.381(9)	1.383(8)	1.378(5)
E′	1.380(6)	1.363(8)	1.364(8)	1.391(8)	1.371(8)	1.375(5)
F	1.357(4)	1.333(7)	1.342(7)	1.357(8)	1.337(7)	1.359(4)
F′	1.359(5)	1.337(7)	1.350(6)	1.346(7)	1.347(7)	1.349(4)
G	1.388(4)	1.382(6)	1.375(6)	1.366(7)	1.382(7)	1.391(4)
G′	1.389(4)	1.356(7)	1.361(6)	1.361(7)	1.378(7)	1.398(4)

alkyl chains on the alcohols reduces the extent of ROH solvation of the 8-NHR moiety augmenting the emission. However, it should be noted that even in hexanol, a significant solvation of the NH occurs since the emission efficiency is much reduced compared to the use of hexane as the solvent.

The quenching of emission by small mole fractions of polar solvents has been well-established in other systems, for example 2-aminonaphthalenes, and explained, inter alia, on the basis of H-bonding to polar excited states.[14] It has been established that the energy of the excited state is the variable of most importance in the emission spectra of such systems, via electronic impact of the substituents, involving enhanced intramolecular charge transfer (ICT). In addition, the steric bulk of the N substituents can have a dramatic impact by removing the planarity of the N atom groups restricting the hemicyanine contribution to the structure. Thus, we were not surprised by the total absence of emission, regardless of solvent, of compound **4**, with two relatively bulky and electron-releasing substituents on the N atom, i.e., both electron-release and steric factors mitigating against efficient emission.[9,14a] According to current ideas as noted above, this latter compound, **4**, should exhibit a solid state structure in which it is not possible to observe a planar structure at the N atom in contrast to those of both **3a** and **3b**. Hence, a structural analysis was performed on all three compounds as well as the previously reported, but not structurally characterized, **2**.

Structural Analysis of 8-Amino-BODIPYs. The new amino-BODIPYS are all crystalline solids, and their structures have been analyzed by single-crystal X-ray diffraction. Full crystal data are presented in the Supporting Information, and selected bond angles and bond lengths are presented in Tables 2 and 3.

There are two isomers of both **3a** and **3b** in their respective asymmetric unit cells, **3a1**(**2**) and **3b1**(**2**). The structures of **2**, **3a1**, and **3b1** together with their side view along the plane of the BODIPY core for **3a1** and **3b1** are illustrated in Figures 8, 9, and 10, respectively.

Table 3. Selected Geometrical Parameters of Compounds 1−4

	1	2a	2b	3a	3b	4
dihedral angle pyrrole rings (deg)	4.2(1)	4.6(1)	5.2(1)	8.0	14.7	30.4
distance B−central 4C plane (Å)	0.152	0.035	0.120	0.319	0.521	
dihedral angle Bodipy-NR_2	4.3(1)	10.0(1)	1.4(1)	11.1	12.7	

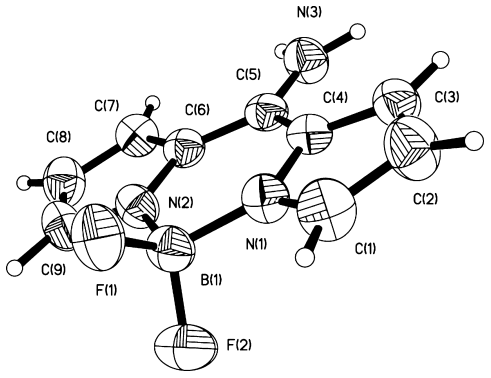

Figure 8. Structure of **2**.

For each of these compounds, as expected, the substituents at the N atom are coplanar; i.e., the structures possess a trigonal planar N atom. This implies that the lone pair of electrons of the N atom are associated with the essentially planar BODIPY core and a reduction in the C8−N bond distance from that expected for a single C−N bond should be observed. Indeed the C8−N bond lengths are in the range 1.31−1.35 Å, typical of bonds intermediate between a C−N and C═N bond, confirming the importance of resonance contribution **B** (Figure 2) for the compounds **2**, **3a**, and **3b**.

dx.doi.org/10.1021/jo302758a | J. Org. Chem. 2013, 78, 4245−4250

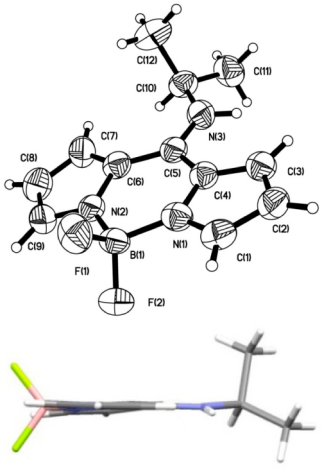

Figure 9. Structure and orientation of **3a1**.

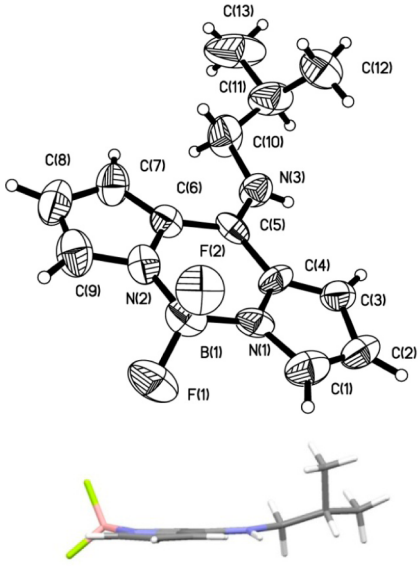

Figure 10. Structure and orientation of **3b1**.

In general, the bond lengths and angles within the BODIPY dipyrrole cores exhibit the same geometric parameters as those examples reported in the literature.[15] There are three important structural parameters for the such compounds, the dihedral angle between the two pyrrole rings, the dihedral angle between the BODIPY core and NR_2 plane, and the distance of the B atom from the central 2C−2N plane, and these data are included in Table 3.

The angle between the pyrrole rings is a key parameter since it is the planarity of the BODIPY core and the extended π-system that is predominantly responsible for the optical properties. Compounds **2**, **3a**, and **3b** have pyrrole−pyrrole dihedral angles of <15°, and since in the case of the NH_2 polymorphs where there is no steric feature of the amino substituents to cause structural irregularities, extended packing forces and structural motifs that exist in the solid state can account for the small dihedral angles noted for these BODIPYs.

The crystal structure and general orientation of compound **4**, illustrated in Figure 11, is distinctive to the general structural features exhibited by **2**, **3a**, **3b**, and other BODIPYs as "expected" from the considerations discussed above.

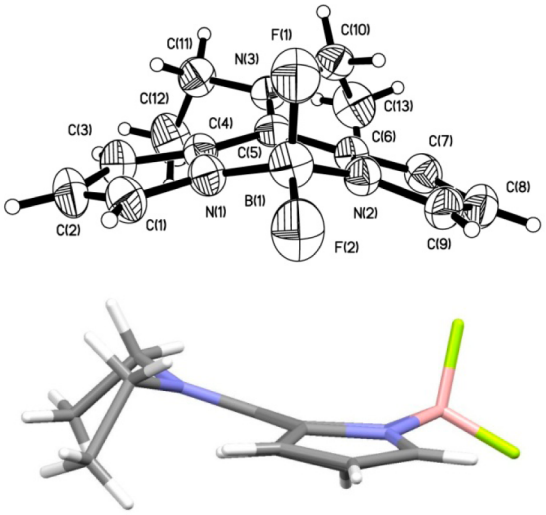

Figure 11. Structure and orientation of **4**.

While the substituents at N are planar there is a pyrrole−pyrrole dihedral angle of 34°, a serious deviation from the previously largely planar arrangements. Further analysis of **4** illustrates that this dihedral angle generates the formation of a "boat" conformation in the six-membered-ring pushing both the nitrogen and boron atoms out of the plane of the four C, N, N, C central atoms by 0.565 and 0.403 Å, respectively, with out-of-plane angles of 15 and 26°, respectively. This behavior demonstrates the significant steric hindrance introduced by the two ethyl groups that are orientated on the same side of the BODIPY molecule, away from the boron group. In the extended solid-state packing diagrams for **3** and **4** there are F···H hydrogen bonding motifs noted that are typical of other unrelated BOFDIP structures and not implicated in the large dihedral angle noted for **4**. Since **4** possesses no emission properties the notion that a planar BODIPY core is needed for fluorescent properties is further reinforced. However, it must be noted that the C8−N bond length in **4** of 1.338(4)Å **2**, is similar to those in both isomers of **3a** and **3b**, Table 2. Clearly, the observation of a shortened C8−N bond by itself does not warrant the immediate assumption of a significant contribution of species **B** (Figure 2) to the structure of the 8-amino-BODIPYs. Our expectation, as delineated above, that the two bulky ethyl groups would not only reduce the emission capacity of the molecule electronically but also prevent the hemicyanine contribution to the structure is vindicated; however, the manner in which this is manifested is perhaps surprising. The planarity of the BODIPY core has been destroyed, to our knowledge the first example of such a structural modification. It seems that the ability of the amino group to place the alkyl substituents orthogonal to the planar BODIPY core, thereby losing a significant planarity at the N atom (i.e., loss of significant sp^2 character) and extending the C8−N bond length, is more energetically demanding than destruction of that planar core. The maintenance of the C8−N multiple bond order seems a paramount consideration in this class of compound. We are currently investigating a range of related substituted-BODIPY systems to further delve into the delicate array of properties, electronic and steric, that modify their properties and structures.

dx.doi.org/10.1021/jo302758a | J. Org. Chem. 2013, 78, 4245−4250

CONCLUSIONS

We have synthesized and completely characterized three new 8-R_2N-BODIPY dyes, R_2 = H^iPr, H^iBu, and Et_2. The study uncovers for the first time a restricted rotation about the C8−N bond that was studied by VT NMR, and further illustrates that the change of substituent on the N atom not only modifies the emission properties of the dyes but also, dramatically, the structure by breaking the planarity of the BODIPY core as observed with **4** (R_2 = Et_2). The emission of the new materials, R_2 = H^iPr and H^iBu, are extremely sensitive to solvent polarity and can readily react to the length of the alkyl chains in a series of alcohols $H(CH_2)_nOH$.

EXPERIMENTAL SECTION

The NMR measurements reported below were obtained using a Varian 300 MHz and/or JEOL ECA 600 MHz spectrometer at room temperature; UV−vis data using a CARY 50 UV−vis spectrometer, and fluorescence spectra using an OLIS DM45 fluorescence spectrometer. The crystal structures of **2**−**4** were determined using a Bruker APEX CCD diffractometer with monochromic MoK_α radiation (λ = 0.71073 Å). Elemental analyses were determined by Galbraith laboratories.

Compounds **2**, **3a**, **3b**, and **4** were synthesized by reacting 8-methylthio-BODIPY (50 mg 0.21 mmol purchased from Cuantico de Mexico, Guanajuato, Mexico) with the corresponding amine in dichloromethane under a nitrogen atmosphere. For compound **2**, ammonium hydroxide solution was used and for **3a**, **3b**, and **4**, 0.2 mmol of *N*-isopropylamine, *N*-isobutylamine, and *N*,*N*-diethylamine were used, respectively. After 5 min of stirring at room temperature silica gel thin-layer chromatography showed the reaction was finished. The product was purified by silica gel column chromatography using 10/90% EtOAc/hexanes. The final products were recrystallized from a dichloromethane/hexane mixture yielding yellow crystals in ∼90% yield.

3a: yellow crystals, yield 88%, 45.8 mg; mp 112−113 °C; ^{1}H NMR ($CDCl_3$) δ 1.44−1.47 (d, 6H, J = 6.18 Hz), 4.40 (septet, 1H, J = 6.18 Hz), 6.34 (s, 1H, broad), 6.51 (s, 2H, broad), 6.90 (s, 1H, broad), 7.16 (s, 1H, broad), 7.53 (s, 1H, broad), 7.67 (s, 1H, broad); $^{13}C\{^1H\}$ NMR ($CDCl_3$) δ 22.3(CH_3), 48.2 (CH), 114.7 (multiple signals, broad), 121.6 (ipso, broad), 123.5 (CH, broad), 125.1 (ipso, broad), 132.5 (CH, broad), 135.19 (CH, broad), 147.5 (ipso). Anal. Calcd for $C_{12}H_{14}N_3BF_2$: C, 57.87; H, 5.67. Found: C, 57.76; H, 5.71.

3b: yellow crystals, yield 91%, 50.0 mg; mp 119−120 °C; ^{1}H NMR ($CDCl_3$): δ 1.08 (d, 6H, J = 6.9 Hz), 2.04 (septet, 1H, J = 6.9 Hz), 3.36 (t, 1H, J = 6.84 Hz), 6.33 (s, 1H, broad), 6.52 (m, 2H, broad), 6.84 (s, 1H, broad), 7.10 (s, 1H, broad), 7.47 (s, 1H, broad), 7.69 (s, 1H, broad); $^{13}C\{^1H\}$ NMR ($CDCl_3$) δ 20.3(CH_3), 28.2 (CH), 54.5 (CH_2), 113.8 (CH, broad), 114.4 (CH, broad), 114.8 (CH, broad), 122.4 (ipso, broad), 123.8 (CH, broad), 125.1 (ipso, broad), 132.4 (CH, broad), 135.6 (CH, broad), 148.4 (ipso). Anal. Calcd for $C_{13}H_{16}N_3BF_2$: C, 59.35; H, 6.13. Found: C, 59.09; H, 6.15.

4: yellow crystals, yield 87%, 47.8 mg; mp 117−118 °C; ^{1}H NMR ($CDCl_3$): δ 1.54−1.56 (t, 6H, J = 6.90 Hz), 4.10−4.11 (q, 4H, J = 6.90), 6.40 (d, 2H, J = 2.16 Hz), 6.97 (d, 2H, J = 3.48 Hz), 7.53 (s, 2H); $^{13}C\{^1H\}$ NMR ($CDCl_3$): δ 13.6 (CH_3), 50.9 (CH_2), 113.0 (CH), 121.6 (CH), 124.2 (ipso), 132.4 (CH), 153.1 (ipso). Anal. Calcd for $C_{13}H_{16}N_3BF_2$: C, 59.35; H, 6.13. Found: C, 59.57; H, 6.19.

ASSOCIATED CONTENT

Supporting Information

^{1}H, ^{13}C, and ^{19}F NMR spectra of **3a**, **3b**, and **4**; solvent-dependent emission of **3a** in $CHCl_3$/THF, $CHCl_3$/acetonitrile, and THF/water mixtures; and crystal and refinement data for **2**, **3a**, **3b**, and **4**. This material is available free of charge via the Internet at http://pubs.acs.org.

AUTHOR INFORMATION

Corresponding Author

*E-mail: kpannell@utep.edu.

Notes

The authors declare no competing financial interest.

ACKNOWLEDGMENTS

We acknowledge the support of the Welch Foundation, Houston, TX.(Grant No. AH-0546), Bridge to the Doctorate Program for a scholarship to R.I.R. (NSF HRD 0832951), the NIH−MARC program, NSF-S-STEM Program, and CON-CyTEG, Guanajuato, Mexico. We also thank Dr. Mahesh Narayan for his assistance with the use of the fluorescence spectrometer.

REFERENCES

(1) Dilek, O.; Bane, S. L. *J. Fluoresc.* **2011**, *21*, 347−354.
(2) Ortiz, M. J.; Garcia-Moreno, I.; Agarrabeitia, A. R.; Duran-Sampedro, G.; Costela, A.; Sastre, R.; Lopez Arbeloa, F.; Banuelos Prieto, J.; Lopez Arbeloa, I. *Phys. Chem. Chem. Phys.* **2010**, *12*, 7804−7811.
(3) (a) Davies, L. H.; Stewart, B.; Harrington, R. W.; Clegg, W.; Higham, L. J. *Angew. Chem.* **2012**, *51*, 4921−24. (b) Wang, D.-P.; Shiraishi, Y.; Hirai, T. *Chem. Commun.* **2011**, *47*, 2673−2675.
(4) Son, H.; Lee, H. Y.; Lim, J.; Kang, D.; Han, W. S.; Lee, S. S.; Jung, J. H. *Chem.—Eur. J.* **2010**, *16*, 11549−11553.
(5) Shiraishi, Y.; Maehara, H.; Sugii, T.; Wang, D.; Hirai, T. *Tetrahedron Lett.* **2009**, *50*, 4293−4296.
(6) Ulrich, G.; Goeb, S.; De Nicola, A.; Retailleau, P.; Ziessel, R. *J. Org. Chem.* **2011**, *76*, 4489−4505.
(7) Gomez-Duran, C. F. A.; Garcia-Moreno, I.; Costela, A.; Martin, V.; Sastre, R.; Banuelos, J.; Lopez Arbeloa, F.; Lopez Arbeloa, I.; Peña-Cabrera, E. *Chem. Commun.* **2010**, *46*, 5103−5105.
(8) Banuelos, J.; Martin, V.; Gomez-Duran, C. F. A.; Cordoba, I. J. A.; Pena-Cabrera, E.; Garcia Moreno, I.; Costelo, A.; Perez-Ojeda, M. E.; Arbeola, T.; Arbeola, I. L. *Chem.—Eur. J.* **2011**, *17*, 7261−7270.
(9) Osorio-Martinez, C. A.; Urias-Benavides, A.; Gomez-Duran, C. F. A.; Banuelos, J.; Esnal, I.; Lopez Albeola, I.; Pena-Cabrera, E. *J. Org. Chem.* **2012**, *77*, 5434−5438.
(10) Goud, T. V.; Tutar, A.; Biellmann, J.-F. *Tetrahedron* **2006**, *62*, 5084−5091.
(11) Ulrich, G.; Ziessel, R.; Harriman, A. *Angew. Chem., Int. Ed.* **2008**, *47*, 1184−1201.
(12) Loudet, A.; Burgess, K. *Chem. Rev.* **2007**, *107*, 4891−4932.
(13) (a) Hong, Y.; Lam, J. W. Y.; Tang, B. Z *Chem. Rev.* **2011**, *40*, 5361−5388. (b) Bandrowsky, T. L.; Carroll, J. B.; Braddock-Wilking, J. *Organometallics* **2011**, *30*, 3559.
(14) (a) Ikeda, N.; Okada, T.; Mataga, N. *B. Chem. Soc. Jpn.* **1981**, *54*, 1025−1030. (b) Seliskar, C. J.; Brand, L. *J. Am. Chem. Soc.* **1971**, 5414. (c) Brand, L. In *Molecular Fluorescence*, 1st ed.; Valeur, B., Ed.; Wiley: New York, 2002; p 218. (d) Liu, Y.-H.; Zhao, G.-J.; Li, G.-Y.; Han, K.-L. *J. Photochem. Photobiol. A* **2010**, *209*, 181−185.
(15) (a) Lu, J.-S.; Ko, S.-B.; Walters, N. R.; Wang, S. *Org. Lett.* **2012**, 5660−5663. (b) Lu, H.; Wang, Q.; Gai, L.; Li, Z.; Deng, Y.; Xiao, X.; Lai, G.; Shen, Z. *Chem.—Eur. J.* **2012**, 7852−7861.